

Effect of Surface Topography of Hydroxyapatite on Human Osteosarcoma MG-63 Cell

CHEN Xiao-Qin¹, CHEN Xue-Ning¹, ZHU Xiang-Dong¹, CAI Bing², FAN Hong-Song¹, ZHANG Xing-Dong¹

(1. National Engineering Research Center for Biomaterials, Sichuan University, Chengdu 610064, China; 2. Analytical and Testing Center, Sichuan University, Chengdu 610064, China)

Abstract: The effect of surface topography of hydroxyapatite (HA) on Human osteosarcoma MG-63 cell lines response was investigated. HA discs with various pore sizes, different pore morphology and distribution were produced by single-axis pressing method. Cell morphology and proliferation were evaluated by scanning electron microscope (SEM) and MTT methods, respectively, and the differentiation potential was assessed by alkaline phosphatase (ALP) activity testing and osteogenic gene expression (RT-PCR). The results showed that the HA discs with macroporous structure ($>200\ \mu\text{m}$) would promote cell adhesion and proliferation, while osteogenic differentiation of MG-63 cells was facilitated by the HA discs with micropore structure ($<100\ \mu\text{m}$). Moreover, the differentiation was also influenced by regularity and distribution of the pore. The irregular and alveolate micropore showed a stronger ability of osteogenic induction than smooth and shallow micropore structure.

Key words: hydroxyapatite; surface topography; osteoinductivity; MG-63 cell

In recent years, the influence of material structure on cell behaviour is a hot spot. Some researchers^[1-4] reported that the material surface structure affected cell behaviour and function, including adhesion^[5], proliferation^[2], metabolism of extracellular matrix^[6-7] and osteogenic differentiation^[3]. However, for calcium phosphate (Ca-P) based materials, the influence of pore structure on cell biological behaviour especially osteogenetic activity, has not yet been fully understood.

Osteoinductive calcium phosphate could be regarded as “intelligent” material which can induce osteogenesis *in vivo*. Previous studies have explored that calcium phosphate materials have the potential for osteoinduction, and such osteoinduction often occur in porous ceramic than dense ones^[8-9]. However, due to the difficulty of getting precise pore structure, the role of pore size and morphology on the osteogenesis is far from clear. What's more, calcium phosphate is mechanically brittle and it is difficult to obtain precise surface topography. Deligianni^[10] and Rosa^[11] reported that surface structure of calcium phosphate ceramic may influence the cell adhesion, proliferation and osteogenic differentiation. But they mostly focused on the surface roughness of material rather than the size or shape of the pores. While studies have shown that

cell proliferation and differentiation were not only related to pore structure at micro-scale, but also to the macro-scale pores. Gonzalez-McQuire^[12] reported that ceramic with the pore size of at least $100\ \mu\text{m}$ can promote cell attachment and proliferation. Our previous study also found that the pore structure of materials would affect the proliferation and ALP expression of MSCs^[13].

To further systematically investigate the effect of material surface topography on osteoblast bioactivity, six hydroxyapatite (HA) discs with different pore size, shape, distribution and even morphology were prepared. MG-63 cells were seeded on the surface of HA discs to investigate the impact of the surface structure on MG-63 cell adhesion and proliferation. Moreover, the gene expressions of Cbfa1 and Col-I were also measured to examine the influence of the material topography on osteogenic differentiation.

1 Material and Methods

1.1 Materials preparation and characterization

The HA discs were prepared according to the previous study^[13]. HA powder (Engineering Research Center in Biomaterials, Sichuan University) was put into a model,

Received date: 2012-01-24; Modified date: 2013-03-19; Published online: 2013-05-28

Foundation item: National Key Technologies R&D Program of China (2011CB606B01); Key Technologies R&D Program of Sichuan Province of China (2012FZ0007)

Biography: CHEN Xiao-Qin(1987-), female, candidate of Master degree. E-mail: chenxiaqinscu@163.com

Corresponding author: FAN Hong-Song, professor. E-mail: hsfan@scu.edu.cn

and certain kind of pore-forming particles were spread on the surface. Then the powder was compacted into HA disc-shaped pellets by single-axis pressing at 100 MPa followed by sintering process to remove the pore-forming particles. Finally, HA discs with different surface topographies were obtained as (1) HA-S: smooth surface, no pore-forming particles used, polished after the sintering process; (2) HA-R50: regular and hemisphere-like micropore, by using polymethyl methacrylate (PMMA) particles with 50 μm diameter as porogen; (3) HA-R200: regular and hemisphere-like macropore structure, by using polystyrene resin (PS) particles with 200 μm diameter as porogen; (4) HA-R500: regular and hemisphere-like macropore, by using polystyrene resin (PS) with 500 μm diameter as porogen; (5) HA-MIR: irregular micropore, by treating HA-S with 1 mol/L hydrochloric acid for 10 min; (6) HA-IR: irregular macropore, by adding NH_4HCO_3 with irregular shape as porogen before pressing.

For different tests, different sizes of discs were prepared: for basic cells test, $\phi 12\text{ mm} \times 2\text{ mm}$; for genetic test: $\phi 20\text{ mm} \times 2\text{ mm}$. After sintering or post treating, the phase composition was assessed by X-ray diffraction (XRD, Dandong Fangyuan DX-1000). The surface topography was characterized by scanning electron microscope (SEM, JSM-5900LM, JEOL, Japan) and Smileview software was used to analyze the surface pore size of the materials.

1.2 Cell adhesion and proliferation

Human osteosarcoma cells (MG-63) were cultured in DMEM medium (Gibco, USA) supplemented with 10% fetal bovine serum and 1% penicillin/streptomycin. The MG-63 cells were seeded at a concentration of 2×10^4 cells/well to the surface of HA discs in 24-well culture plates (Falcon, USA) and cells cultured on blank wells were used as a control group.

Cell morphology on different material surface was observed by SEM at day 3. MTT assay was used to measure cell viability after being cultured on the discs for 2, 4 and 6 d. The absorbance of the resulting solution was measured at 570 nm using a multi-detection microplate reader (Bio-Rad 550).

1.3 Alkaline phosphatase activity

The activity of intracellular alkaline phosphatase (ALP) was measured with a SensoLyte pNPP Alkaline Phosphatase Assay Kit (AnaSpec, Inc.). Aliquots of 500 μL of cell lysate were obtained according to the procedure de-

scribed and mixed with an equal amount of pNPP working solution in 96-well microplate. Mixtures were then incubated for 30 min at 37°C . The reaction was stopped by addition of 50 μL stop solution to each well and the resulting optical densities were measured at 405 nm with a microplate photometer (Thermo Multiskan MK3, USA). Measurements were compared to an alkaline phosphatase standard and normalized using the total protein amounts which were measured with a BCA protein assay kit (Pierce, USA).

1.4 Osteogenic gene expression

The expressions of osteogenesis-related genes of Cbfa1 and Collagen-I were investigated by quantitative real-time reverse transcriptase-polymerase chain reaction (qRT-PCR). After 3 d, total RNA was extracted from samples using Trizol reagent (Invitrogen, USA) following the manufacturer's protocol. And then it is converted into complementary DNA (cDNA) using ReverTra Ace® qPCR RT Kit (TakaRa, Japan). The sequences of primers for core-binding factor $\alpha 1$ (Cbfa1), collagen I (Col-I) and GAPDH genes were given in Table 1. A quantitative real-time PCR reaction was performed using CFX96TM real-time PCR detection system (Bio-Rad, CFX960) with SsoFastTM EvaGreen® Supermix (Bio-Rad). GAPDH was used as the housekeeping gene to normalize results.

2 Results and Discussion

2.1 XRD analysis

Figure 1 showed the XRD patterns of the prepared HA samples. The six samples exhibited the same typical phase composition of hydroxyapatite, which indicated that the porogens were successfully removed by calcination and the processing procedures did not change the phase composition of samples.

2.2 Surface characterization of materials

SEM images of surface structure of HA discs were shown in Fig. 2(A-F), and the measured average pore size was listed in Table 2. The SEM images showed that a layer of regular and closely connected hemispherical shallow pores with different pore size was covered on the surface of sample HA-R50, HA-R200 and HA-R500. While on the surface of HA-IR, the shallow pores were

Table 1 Primers sequences for target genes

Symbol	The left primers	The right primers	Product size
Col- I	5'-CAAGAACCCCAAGGACAAGAG-3'	5'-CTTGCAAGTGGTAGGTGATGTTC-3'	169 bp
Runx2 (Cbfa1)	5'-CACTGGCGCTGCAACAAGA-3'	5'-CATTCCGGAGCTCAGCAGAATAA-3'	127 bp
GADPH	5'-GCACCGTCAAGGCTGAGAAC-3'	5'-TGGTGAAGACGCCAGTGGA-3'	138 bp

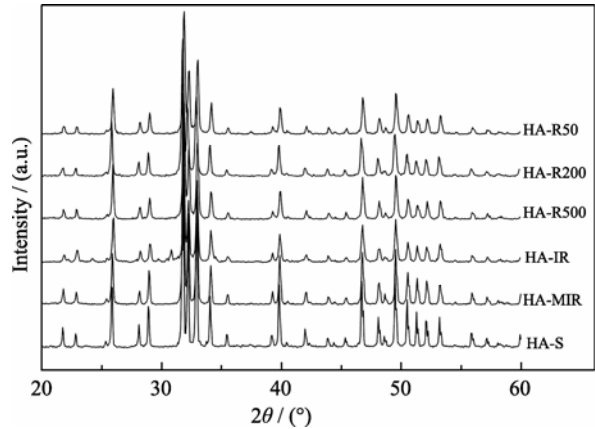


Fig. 1 XRD patterns of the prepared HA

extremely irregular and disorderly distributed with an average pore size of 473.7 μm which was similar to HA-R500. HA-MIR showed a honeycomb multi-level irregular pore structure with the average pore size of about 30 μm while the HA-S surface was dense and smooth.

The result indicated that HA discs with different surface topography were successfully constructed by using single-axis pressing methods with the assistance of proper porogen. The size and morphology could be designed evenly and precisely. Obviously, by controlling the size and morphology of porogen, the pores with corresponding size and morphology were fabricated precisely as shown in Fig. 2 (HA-R50, HA-R200, HA-R500

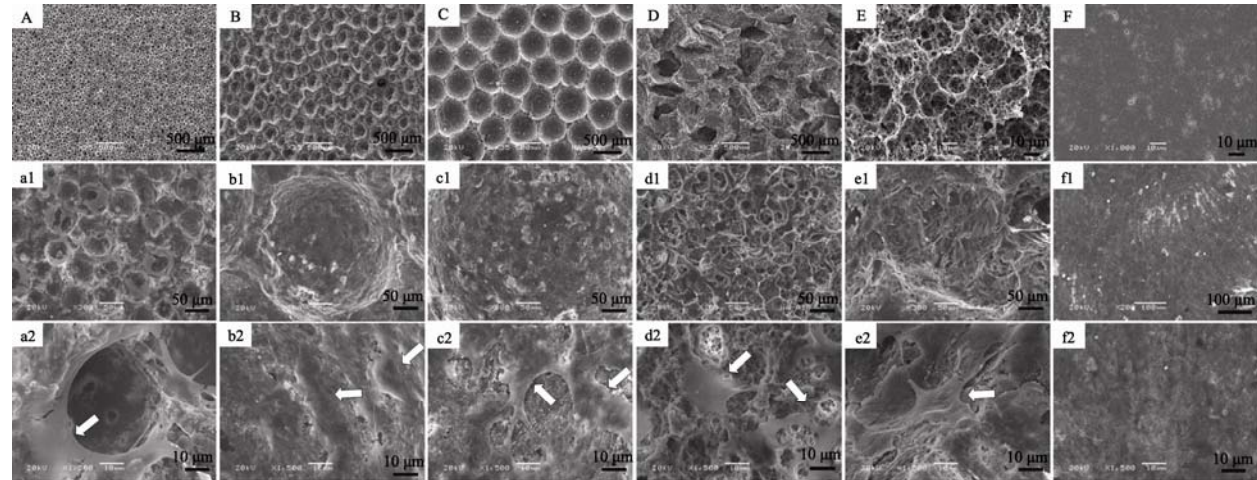


Fig. 2 SEM images of HA surface topography without cells (A-F) and with MG-63 cells on HA surface (a1-f2). Arrows: Cells. (A, a1) HA-R50, (B, b1), HA-R200, (C, c1) HA-R500, (D, d1) HA-IR, (E, e1) HA-MIR and (F, f1) HA-S (a2), (b2), (c2), (d2), (e2) and (f2) are the higher magnification images of (a1), (b1), (c1), (d1), (e1) and (f1), respectively

Table 2 Pore size on the surface of HA materials(mean±SD)

Sample	HA-R50	HA-R200	HA-R500	HA-IR	HA-MIR
Mean pore size/ μm	52.96±8.67	203.6±36.5	507.7±30.2	473.7±133.7	27.6±5.91

and HA-IR). The advantage of this method is that surface topography of the ceramics can be easily designed at the scale from 50 μm to 500 μm . Since it is difficult to get proper pores under 50 μm , acid erosion is employed to obtain a micropore structure in the range of 20–30 μm as shown in sample HA-MIR.

2.3 Cell proliferation

Figure 3 showed the cell viability of MG-63 cells cultured on different HA discs after 2, 4 and 6 d. Obvious cell proliferation was observed on all of the six discs, indicating that all the materials were biocompatible and could support cell proliferation which was consistent with the previous studies^[14]. However, the data also showed that the proliferation behavior varied with the surface structure of the ceramics.

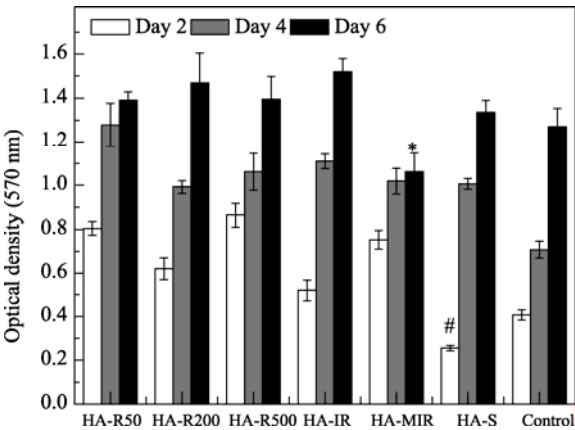


Fig. 3 Cell proliferation on different surface structure of HA evaluated by MTT
HA-S shows lower viability compared to other materials (#: $p < 0.05$) at day 2 and HA-MIR shows lower than others at day 6(*: $p < 0.05$)

MG-63 cells on HA-S showed statistically lower viability comparing to other materials at the early days. But it increased dramatically with prolonging the culture time which was similar to the control group, indicating that a smooth surface was more conducive to cell proliferation. This may be due to a fact that smooth surface have less stimulation on cell skeleton, and cells can attach, spread easily, thus the proliferation process was not significantly affected.

Compared with other groups, MG-63 cells on HA-R50 and HA-MIR showed different proliferation trend: The cells proliferated rapidly at day 2 and day 4 while gradually slowed down at day 6. This may be related to the surface pore structure and pore size. For both the groups, the pore size was less than 100 μm which was similar to the size of MG-63 cell. This micropore would promote cell proliferation at the early days and achieved a maximum value at day 4, while on the sixth day when the cells showed contact inhibition, cell proliferation slowed down. The lowest cell viability of HA-MIR group at day 6 may be related to its irregularly honeycombed porous structure.

2.4 Cell morphology

Cell morphology was examined by SEM after 3 d cell seeding to reveal the cell adhesion on the surfaces of the materials. As shown in Fig. 2 (a1-f1, a2-f2), it was evident that cells spread well on all materials.

Corresponding to the different cell proliferation trend on HA-R50 and HA-MIR, the cell adhesion on these two groups were also different with other groups. For both materials, cells closely attached on the edge of the pores and extended to the center of the pore, trying to cover the micropores. While for other groups, cells closely attached to the pore wall and growth in monolayer. Single cells exhibited a polygonal or star-shaped morphology with many extended pseudopodia when firmly attached to the material substrate. Moreover, cells on materials have been connected into a sheet covering the surface of the material especially on the HA-R200 and HA-S. It is difficult to observe a single cell morphology.

The results clearly proved that cell morphology varied with the surface structure of material. Cells on materials with smaller surface pores showed obviously different morphology with that of bigger surface pores. As MG-63 cell belongs to the family of cells that need an appropriate substrate to attach to so that they can get fully stretched^[15]. Therefore, for group HA-200, HA-500 and HA-IR, when the pore size is much larger than MG-63 cells, it can provide a proper base for cell attachment where cells can spread well on the pore wall. While for HA-R50 and HA-MIR, the wall surface of pore were much smaller than cells and the cells were likely to attach on the edge of the pore and cover the micropores.

2.5 Alkaline phosphatase activity (ALP)

Figure 4 displayed the ALP activity of MG-63 affected by the surface topography. Generally, the ALP activity of each group increased with the culture time. HA-MIR group had the highest ALP activity, followed by the HA-S, HA-R50 and HA-R200 group, while HA-R500 and HA-IR group owned the lowest value. It can be inferred that surface structure of HA affected the intracellular alkaline phosphatase activity significantly.

ALP expression served as an important index of early osteoblast differentiation^[16]. The highest ALP expression of cells on HA-MIR indicated that the small and shallow micropore structures might have the ability to facilitate the early differentiation process of MG-63. The higher ALP activity on HA-S, HA-R50 and HA-R200 groups also indicated a higher degree of differentiation than cells on HA-R500 and HA-IR groups.

HA-R500 and HA-IR groups showed high cell viability while the expression of alkaline phosphatase was very low. This might be due to a greater surface area of the two materials would provide a larger number of cell adhesion points and allow the continuous proliferation of cells while cell differentiation was inhibited. In comparison, HA-R200 had a moderate pore structure, not only accommodated the appropriate number of cells, but also can promote cell differentiation, and therefore increased alkaline phosphatase activity.

Among all the groups, HA-MIR and HA-R50 groups have the highest alkaline phosphatase activity, indicating that pore size (less than 100 μm) at cell-scale would promote osteogenic differentiation of MG-63 cells. For HA-S and the control group, a high ALP expression was also found which means a spontaneous osteogenic differentiation of MG-63 cells, indicating that the smooth surface have no significant effect on osteogenic differentiation process. However, it still required further confirmation on the cellular and molecular level by using RT-PCR means.

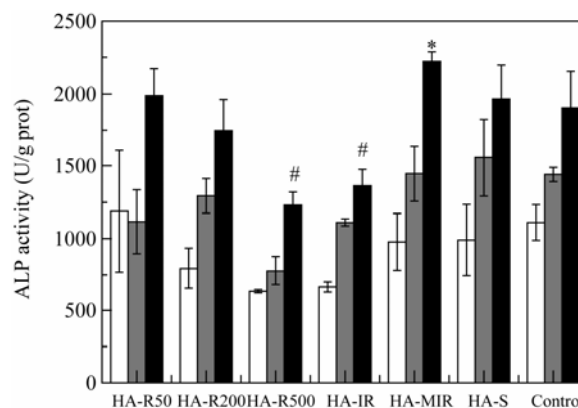


Fig. 4 Alkaline phosphatase (ALP) activity of MG-63 on HA materials after 3, 6 and 9 d
HA-MIR has the highest ALP activity (*, $p < 0.05$); HA-IR has the lowest ALP activity at day 9(#, $p < 0.05$)

2.6 Osteogenic gene expression

The expression of Cbfa1 and Col- I genes of MG-63 cells seeded on the HA was shown in Fig. 5. The surface structure of HA had great influence on the expression of Cbfa1. There was a low expression of Cbfa1 genes in HA-R500 and HA-IR compared with HA-S which had a smooth surface. Much higher Cbfa1 gene expression was found in HA-R50 and HA-R200, and HA-MIR was the highest. The result was consistent with the ALP activity. In contrast, the expression of Col- I showed almost similar level on all the materials, indicating that the surface structure of HA had little influence on the expression of Col- I gene. This might be related to the different signal pathway that modulated the expression of Col- I and Cbfa1 genes.

Cbfa1 is an osteoblast-specific transcription factor and a key regulator of osteoblast differentiation and function. The expression of Cbfa1 indicates the early osteoblast differentiation of the cells^[17]. The significantly higher expression of Cbfa1 in HA-MIR, HA-R50 and HA-R200, which was consistent with that of ALP activity, indicating that these surface topographies were more likely to up-regulate Cbfa1 expression thus supporting adherent cells differentiation along osteogenic lineage.

According to the ALP activity and Cbfa1 gene expression, it can be concluded that the osteoblast differentiation of MG-63 was highly affected by the surface topography of materials. HA-MIR showed a highest differentiation, followed by HA-R50, HA-200, HA-S, HA-IR and HA-R500. This trend was contrary to that of cell proliferation. The low Cbfa1 expression of HA-R500 and HA-IR might be due to the large pore size with little stimulation on cell differentiation, meanwhile, the large pores could promote cell division, growth and prolong the proliferative phase of MG-63. Finally the osteogenic differentiation of cells was inhibited.

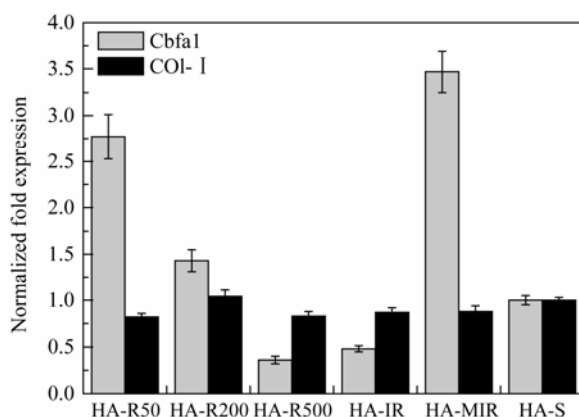


Fig. 5 Cbfa1 and Col- I gene expressions of the MG-63 cells cultured on HA for 3 d

GAPDH is used as the house-keeping gene to normalize results

However, other three groups with small pore size ($<200\ \mu\text{m}$) had positive effect on cell differentiation. The expression of Cbfa1 gene increased with the decrease of pore size. MG-63 cells could be more easily identified by small pore and promote the osteogenic differentiation. On the other hand, the irregular alveolate surface of HA-MIR improved the expression of Cbfa1.

3 Conclusion

The surface structure of HA bioceramics has a certain impact on osteogenic differentiation of MG-63 cells. The micropore structure on HA surface ($<100\ \mu\text{m}$, HA-R50 and HA-MIR) was more likely to promote osteogenic differentiation of MG-63 cells while the macropore ($>200\ \mu\text{m}$, HA-500 and HA-IR) favored the cell proliferation. Moreover, the regularity and distribution of the pores influenced the osteogenic differentiation of MG-63 cells. For similar pore size, irregular and alveolate micropore structures (HA-MIR) showed stronger ability of osteogenic induction than the smooth and shallow structures (HA-R50).

References:

- [1] Boyan B D, Sylvia V L, Liu Y, *et al.* Surface roughness mediates its effects on osteoblasts *via* protein kinase A and phospholipase A₂. *Biomaterials*, 1999, **20**(23/24):2305–2310.
- [2] Mustafa K, Wroblewski J, Lopez B S, *et al.* Determining optimal surface roughness of TiO₂ blasted titanium implant material for attachment, proliferation and differentiation of cells derived from human mandibular alveolar bone. *Clinical Oral Implants Research*, 2008, **12**(5):515–525.
- [3] Lincks J, Boyan B, Blanchard C, *et al.* Response of MG-63 osteoblast-like cells to titanium and titanium alloy is dependent on surface roughness and composition. *Biomaterials*, 1998, **19**(23):2219–2232.
- [4] Yang F, Dong W, He F, *et al.* Osteoblast response to porous titanium surfaces coated with zinc-substituted hydroxyapatite. *Oral Surgery, Oral Medicine, Oral Pathology and Oral Radiology*, 2012, **113**(3):313–318.
- [5] Zhe W, Zhan-Wen X, Hong-Song F, *et al.* Fabrication of micro-grooved patterns on hydroxyapatite ceramics and observation of earlier response of osteoblasts to the patterns. *Journal of Inorganic Materials*, 2013, **28**(1):51–57.
- [6] Boyan B, Bonewald L, Paschalis E, *et al.* Osteoblast-mediated mineral deposition in culture is dependent on surface micro-topography. *Calcified Tissue International*, 2002, **71**(6): 519–529.
- [7] Lohmann C, Bonewald L, Sisk M, *et al.* Maturation state

- determines the response of osteogenic cells to surface roughness and 1, 25-dihydroxyvitamin D₃. *Journal of Bone and Mineral Research*, 2000, **15**(6):1169–1180.
- [8] Yuan H, Kurashina K, de Bruijn J D, *et al.* A preliminary study on osteoinduction of two kinds of calcium phosphate ceramics. *Biomaterials*, 1999, **20**(19):1799–1806.
- [9] Wu C, Chang J, Zhai W, *et al.* Porous akermanite scaffolds for bone tissue engineering: preparation, characterization, and *in vitro* studies. *Journal of Biomedical Materials Research Part B: Applied Biomaterials*, 2006, **78**(1):47–55.
- [10] Deligianni D D, Katsala N D, Koutsoukos P G, *et al.* Effect of surface roughness of hydroxyapatite on human bone marrow cell adhesion, proliferation, differentiation and detachment strength. *Biomaterials*, 2000, **22**(1):87–96.
- [11] Rosa AL, Beloti MM, van Noort R. Osteoblastic differentiation of cultured rat bone marrow cells on hydroxyapatite with different surface topography. *Dental Materials*, 2003, **19**(8):768–772.
- [12] Gonzalez-McQuire R, Green D, Walsh D, *et al.* Fabrication of hydroxyapatite sponges by dextran sulphate/amino acid templating. *Biomaterials*, 2005, **26**(33):6652–6656.
- [13] Chen X N, Zhu X D, Fan H S, *et al.* Rat bone marrow cell responses on the surface of hydroxyapatite with different topography. *Key Engineering Materials*, 2008, **361–363**:1107–1110.
- [14] Hui-Tao L, Wei Z, Xiong L, *et al.* Research on preparation and biological properties of dense hydroxyapatite spheres. *Journal of Inorganic Materials*, 2013, **28**(1):40–44.
- [15] Billiau A, Edy V, Heremans H, *et al.* Human interferon: mass production in a newly established cell line, MG-63. *Antimicrobial Agents and Chemotherapy*, 1977, **12**(1):11–15.
- [16] Lian J B, Stein G S. Concepts of osteoblast growth and differentiation: basis for modulation of bone cell development and tissue formation. *Critical Reviews in Oral Biology & Medicine*, 1992, **3**(3):269–305.
- [17] Schneider G, Perinpanayagam H, Clegg M, *et al.* Implant surface roughness affects osteoblast gene expression. *Journal of Dental Research*, 2003, **82**(5):372–376.

羟基磷灰石表面形貌对人成骨肉瘤细胞生物学性能的影响

陈晓琴¹, 陈雪宁¹, 朱向东¹, 蔡兵², 范红松¹, 张兴栋¹

(四川大学 1. 国家生物医学材料工程技术研究中心; 2. 分析测试中心, 成都 610064)

摘要: 本文研究了羟基磷灰石(HA)表面形貌对人成骨肉瘤细胞(MG-63)生物学性能的影响。通过单轴压片技术与粒子占位法相结合控制陶瓷表面孔尺度、形态及分布, 从而获得具有不同表面孔结构的 HA 陶瓷材料。将材料与 MG-63 共培养, 通过扫描电子显微镜(SEM), MTT 检测法表征材料表面形貌对细胞的黏附和增殖影响, 并通过碱性磷酸酶活性(ALP)检测和实时荧光定量(RT-PCR)技术探讨了 HA 陶瓷材料的表面结构对 MG-63 成骨分化的诱导作用。结果表明, 大孔结构(孔径大于 200 μm)更有利于细胞的黏附和增殖, 而小孔结构(孔径小于 100 μm)能促进细胞的成骨分化。孔形貌和孔分布也能影响细胞的生物功能, 相同尺度的孔径, 不规则蜂窝状的多级微孔结构比光滑孔壁的浅孔结构更能诱导细胞的成骨分化。

关键词: 羟基磷灰石; 表面形貌; 骨诱导性; MG-63 细胞

中图分类号: R318; TB321

文献标识码: A